



## Full Length Article



# Green synthesis of gold nanoparticles via *Artocarpus odoratissimus* peel extract for potential applications of optical filter and catalytic degradation

Eleen Dayana Mohamed Isa<sup>a</sup>, Siti Rahmah Aid<sup>b,\*</sup>, Roshafima Rasit Ali<sup>a</sup>, Yutaka Asako<sup>c</sup>, Kamyar Shameli<sup>d</sup>, Nur Farhana Arissa Jonny<sup>b</sup>, Aina Hiyama Zazuli<sup>b</sup>, Siti Husnaa Mohd Taib<sup>a</sup>, Mostafa Yusefi<sup>a</sup>

<sup>a</sup> Department of Chemical and Environmental Engineering, Malaysia-Japan International Institute of Technology, Universiti Teknologi Malaysia, Jalan Sultan Yahya Petra, 54100 Kuala Lumpur, Malaysia

<sup>b</sup> Department of Electronic Systems Engineering, Malaysia-Japan International Institute of Technology, Universiti Teknologi Malaysia, Jalan Sultan Yahya Petra, 54100 Kuala Lumpur, Malaysia

<sup>c</sup> Department of Mechanical Precision Engineering, Malaysia-Japan International Institute of Technology, Universiti Teknologi Malaysia, Jalan Sultan Yahya Petra, 54100 Kuala Lumpur, Malaysia

<sup>d</sup> School of Medicine, Technical University of Munich, 81675 Munich, Germany

## ARTICLE INFO

## Keywords:

Green synthesis  
Gold nanoparticles  
Optical filter  
Catalytic  
*Artocarpus odoratissimus*

## ABSTRACT

Gold nanoparticles (Au NPs) were synthesized via a green synthesis method, utilizing the peel extract of *Artocarpus odoratissimus* as both the reducing and capping agent. This study investigates the impact of peel extract concentration (ranging from 0.002 to 0.012 g/mL) and reaction temperature (including room temperature, 45 °C, and 75 °C) on the properties of the synthesized Au NPs. Various characterization techniques, such as UV-Visible spectrophotometry, transmission electron microscopy (TEM), Fourier Transform infrared spectroscopy (FTIR), X-ray diffractometry (XRD), and zeta potential analysis, were employed to analyze the synthesized samples. UV-Visible spectroscopy revealed absorption peaks of the Au NPs around 533–537 nm, varying with synthesis parameters, while TEM analysis indicated particle sizes ranging from 12 to 25 nm. XRD analysis confirmed the formation of Au NPs, with diffraction peaks aligning well with the standard. FTIR analysis suggested interactions between phytochemicals and Au NPs, contributing to their reduction and size control. The synthesized Au NPs exhibited remarkable optical filtering capability, with up to 87 % transmittance in the 751–1126 nm spectral range and significant absorbance in the lower wavelength region (300–751 nm). Additionally, catalytic studies revealed that Au NPs accelerated the degradation of rhodamine B dye, 0.0795 min<sup>-1</sup>, compared to 0.0445 min<sup>-1</sup> without Au NPs. These findings underscore the potential of Au NPs for use in hybrid photovoltaic-thermal systems as filters, where transmitted light can be harvested for photovoltaic energy generation while absorbed light can be utilized for the thermal aspect. Moreover, Au NPs offer promise for improving wastewater quality by enhancing pollutant degradation.

## 1. Introduction

*Artocarpus odoratissimus*, commonly known as tarap fruit, thrives in the tropical climate of Borneo Island and belongs to the same genus as jackfruit and breadfruit, exhibiting a visual resemblance to both (Abu Bakar and Abu Bakar, 2018, Xia et al., 2023). With its widespread presence, various parts of this fruit tree are harnessed for traditional medicinal purposes, offering remedies for ailments such as diabetes,

diarrhea, malaria, tapeworm infection, and even serving as an antidote for insect stings (Yulianti et al., 2022). While the flesh of the fruit is the consumable part, its peel and seeds are typically discarded as waste. Recent statistics from the Philippines Statistic Authority reveal an annual generation of 26 metric tons of waste from these fruit peels and kernels (Alvarado, 2023). Remarkably, a study led by Abu Bakar and colleagues uncovered the remarkable antioxidant and anticancer properties residing in the kernel and peel due to their high phenolic content,

\* Corresponding author.

E-mail addresses: [eleendayana@utm.my](mailto:eleendayana@utm.my) (E.D. Mohamed Isa), [sitirahmah.aid@utm.my](mailto:sitirahmah.aid@utm.my) (S.R. Aid), [roshafima@utm.my](mailto:roshafima@utm.my) (R. Rasit Ali), [y.asako@utm.my](mailto:y.asako@utm.my) (Y. Asako), [sitihusnaa@utm.my](mailto:sitihusnaa@utm.my) (S.H. Mohd Taib).

<https://doi.org/10.1016/j.jksus.2024.103209>

Received 5 January 2024; Received in revised form 7 April 2024; Accepted 11 April 2024

Available online 12 April 2024

1018-3647/© 2024 The Authors. Published by Elsevier B.V. on behalf of King Saud University. This is an open access article under the CC BY-NC-ND license (<http://creativecommons.org/licenses/by-nc-nd/4.0/>).

surpassing that of the fruit flesh (Fadzelly Abu Bakar et al., 2010). High antioxidant activity suggests the potential of fruit waste to act as a reducing agent for metal ions, converting them into metallic elements. Hence, exploring the utilization of tarap fruit waste, particularly the peel, as a natural reductant for gold nanoparticles' (Au NPs) production will be the main aim in this research. Fig. 1 shows the physical appearance of *Artocarpus odoratissimus*.

Au NPs popularity is on the rise in recent research due to their desirable properties, including tunable morphology and size, excellent photothermal conversion, good chemical and photo-stability and ease of functionalization (Wu et al., 2019). Synthesizing Au NPs typically involves three main methods: physical, chemical and green synthesis. The physical method requires specialized equipment and high energy, such as laser ablation or thermal evaporation, making it less desirable. In contrast, the chemical method relies on toxic chemicals, such as sodium borohydride, commonly used as a reducing agent in nanoparticle production, which poses environmental risks due to the release of toxic gases upon decomposition (Abid et al., 2022). The green synthesis approach emerges as a preferred alternative, given its cost effectiveness and utilization of environmentally friendly products, such as plant extracts, for reducing gold salt to Au NPs (Punnoose and Mathew, 2022). Previous studies have successfully demonstrated Au NPs synthesis using plant extracts from various sources, including *Amaranthus tricolor* leaves extract with the aid of microwave (Punnoose et al., 2022), orange fruit extract (Cortez-Valadez et al., 2021) root of banana tree extract (Das and Biswas, 2023), and extract from waste fruit peels (Pechyen et al., 2021).

Energy and water represent two vital resources currently experiencing high demand. The demand for energy has surged exponentially, propelled by the burgeoning global population and rapid technological advancements. Projections suggest that by 2040, energy demand will escalate by approximately 30 % compared to current levels (Kumar et al., 2021). However, this surge is exacerbated by the rapid depletion of fossil fuels, the predominant energy source, posing a significant risk of unmet demand. Concurrently, the demand for clean water is escalating in tandem with population growth. Regrettably, the availability of clean water sources faces considerable jeopardy due to pollution.

Consequently, there is a pressing need for solutions to address both challenges. Among these solutions, Au NPs hold promise as a potential remedy.

To address the escalating energy demand, researchers have redirected their efforts toward harnessing renewable sources, particularly solar energy. Among the most efficient systems for solar energy harvesting is photovoltaic thermal technology (PVT). Recent advancements in PVT technology have sparked considerable interest in spectral beam splitting. This technique holds promise for enhancing solar energy harvesting by selectively filtering the solar spectrum for solar-to-electricity conversion, while diverting the remaining spectrum to thermal conversion (Han et al., 2022). Au NPs exhibit remarkable potential as efficient optical filters, owing to a phenomenon known as localized surface plasmon resonance (LSPR), which enhances light absorption (Duan et al., 2019, Kamyar et al., 2021). Beyond their application in energy systems, Au NPs also demonstrate catalytic prowess in degrading pollutants in water, offering a promising solution to address water scarcity issues (Sivakavinesan et al., 2022).

In this study, Au NPs were synthesized using *Artocarpus odoratissimus* peel extract. The impact of plant extract's concentration and reaction temperature on the properties of Au NPs were studied. The best Au NPs were selected for further investigation as optical filters for silicon and germanium PV cells and for degrading rhodamine B. These findings are significant for advancing SDGs 6 and 7, related to clean water, sanitation, and affordable clean energy.

## 2. Materials and methodology

### 2.1. Materials

Fresh *Artocarpus odoratissimus* ripe fruit was purchased from local market in Seri Kembangan, Selangor, Malaysia and the fruit parts were separated to the flesh, seed and peel where the peel was used as starting material. Analytical grade gold (III) chloride trihydrate ( $\text{HAuCl}_4 \cdot 3\text{H}_2\text{O}$ ) and sodium borohydride ( $\text{NaBH}_4$ ) were purchased from Sigma-Aldrich, USA. Analytical grade rhodamine B (RhB) and ethanol were purchased from R & M Chemicals, Malaysia.

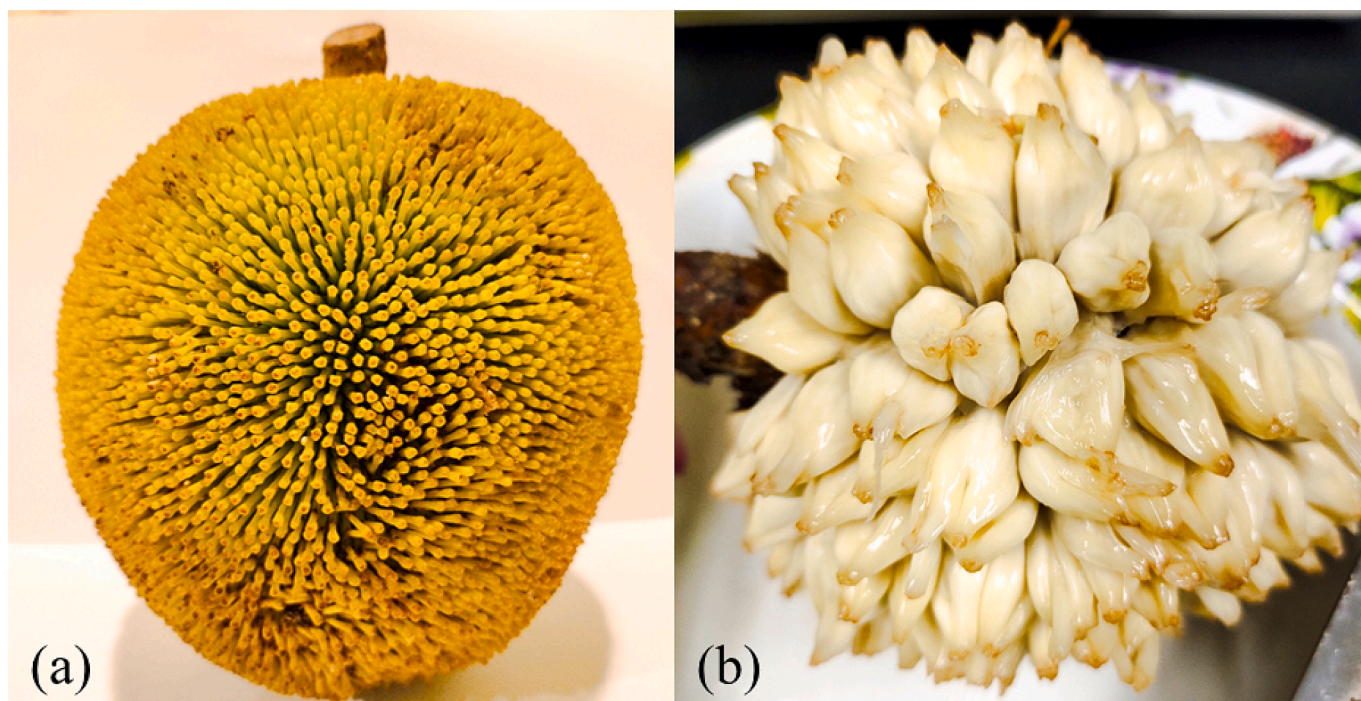


Fig. 1. (a) *Artocarpus odoratissimus* fruit and (b) the flesh of the fruit.

## 2.2. Preparation of the *Artocarpus odoratissimus* peel extract

The fruit was thoroughly washed under running tap water to remove dirt and washed again with distilled water. The fruit was then separated to flesh, seed, and peel. The peels were dried in the oven at 60 °C for 24 h. The dried peel was grinded to fine powder and stored in deep freezer at -20 °C. Soxhlet extraction process was utilized to collect the peel extract. 50 g of powdered peel was extracted using 200 mL of 1:1 ratio of ethanol and water as the solvent and the extraction was conducted for 6 h. The extract was then filtered and concentrated using rotary evaporator. The concentrated peel extract was dried in the oven at 60 °C overnight. The dried extract was collected and stored in the desiccator before further usage.

## 2.3. Synthesis of gold nanoparticles

A certain amount of dried extract was dissolved in 10 mL water and added to 30 mL of 0.5 mM HAuCl<sub>4</sub> solution. The mixture was stirred (500 rpm) until the reaction is complete which is indicated by the change of the solution color. The effect of plant extract concentration was studied by varying the concentration to 0.002, 0.004, 0.008 and 0.012 g/mL. The effect of temperature was also studied by varying the synthesis temperature to room temperature, 45 °C and 75 °C.

## 2.4. Characterization

The absorbance of synthesized Au NPs was collected on Shimadzu UV-2600 spectrophotometer. Fourier transform infrared (FTIR) spectra were obtained using Shimadzu IRTracer-100. The X-ray diffraction (XRD) analyses were conducted using the Analytical X'pert Pro MPD diffractometer with Cu K $\alpha$  radiation ( $\lambda = 1.5406$ ) in the range of 10°-90°. The stability of synthesized samples was evaluated through zeta potential analysis via Particulate System Nano-Plus Zeta/Nano Particle Analyzer. The particle morphology were determined through high-resolution transmission electron microscopy (HRTEM) using JOEL JEM-2100F.

## 2.5. Optical characteristic of Au NPs

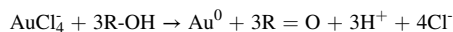
To study the capability of Au NPs for spectral splitting in PVT system, the transmittance of solution is a key parameter in determining the performance of the system. Therefore, spectroscopic analysis of fluids with different concentrations of Au NPs was conducted. The solar spectral transmittance (300–1400 nm) of base fluid (water), Au NPs solutions with concentration of 20, 40 and 60 ppm were tested using Shimadzu UV-2600 spectrophotometer. The transmittance of the solutions was matched with single crystal silicon and germanium cell PV modules. The range used to generate electricity for silicon PV cell is between 751 and 1125 nm and for germanium PV cell is between 1270 and 1906 nm while the remaining energy range is used to generate thermal energy (Taylor et al., 2012, Xia et al., 2023). Therefore, the solution with the highest transmittance between the desired range and lowest transmittance in the other range is the best option to be used as spectral splitting in PVT system.

## 2.6. Catalytic reduction of rhodamine B dye

The catalytic study was studied through degradation of model dye, RhB, with NaBH<sub>4</sub> as the reducing agent and synthesized Au NPs as the catalyst. 3 mL of 10 ppm RhB dye solution was prepared and 50  $\mu$ L of Au NPs solution was added and the mixture was incubated for 30 min to reach adsorption-desorption equilibrium. Then 0.5 mL of 0.6 M NaBH<sub>4</sub> was added to the mixture and the absorbance was recorded at 554 nm using UV-Visible spectrophotometer at different time intervals (0–50 min).

## 3. Results and discussion

*Artocarpus odoratissimus* peel extract functions as both a reducing and stabilizing agent in Au NPs synthesis. Within the initial five minutes, the mixture of the peel extract and gold salt solution transitioned from a brownish color to a red wine hue, indicating the formation of Au NPs (Fig. 2). The peel extract can reduce the gold salt to Au NPs without pH alteration, attributed to its high flavonoid and total phenolic contents, as reported in previous work (Abu Bakar et al., 2015). Phenolic compounds like ferulic, chlorogenic and p-coumaric acids contain hydroxyl groups which potentially aid in the bioreduction and stabilization of gold salts to Au NPs. The formation mechanism is illustrated in Fig. 2 (d). During the reaction, the hydroxyl undergoes oxidation while the gold ions are reduced to Au NPs, represented by the following equation (Lee et al., 2017).



### 3.1. Ultraviolet-visible spectroscopy analysis

In addition to monitoring the physical changes in the solution as the reaction progresses, UV-Visible spectroscopy analysis confirmed the formation of Au NPs. A single peak within the 500–600 nm range, attributed to the surface plasmon resonance (SPR) effect of Au NPs, was observed, indicating their monodispersity (Nayak et al., 2022). The position of Au NPs SPR peak in the UV-Vis spectrum varies with different parameters (Rokkarukala et al., 2023). In this work, the impact of plant extract concentration on Au NPs formation was investigated, and the spectra are depicted in Fig. 3 (a). A single peak representing the Au NPs was observed, shifting from 533 nm (at 0.002 g/mL) to 537 nm with an increase in plant extract concentration. This red-shift of the SPR peak may be due to an increase in the particle size of Au NPs (Shanmugam, 2022). Furthermore, as the extract concentration increased from 0.002 g/mL to 0.008 g/mL, the absorbance of Au NPs also increased. However, further increments did not yield significant changes in absorbance intensity, suggesting that at an extract concentration of 0.008 g/mL, all the gold salt was effectively reduced to Au NPs the time required to reach maximum absorbance decreased from 150 min for 0.002 g/mL to 20 min for 0.008 g/mL and 0.012 g/mL. Based on these findings, we selected an extract concentration of 0.008 g/mL to examine the impact of reaction temperature, illustrated in Fig. 3 (b). Overall, minor changes were observed in the spectra as the reaction temperature increased. The SPR peak position exhibited only a slight red-shift, from 537 nm to 538 nm, at 75 °C. This phenomenon may indicate an increase in particle size, expected as nanoparticle growth predominates at elevated temperatures, resulting in larger nanoparticles (Lee et al., 2019). However, the discrepancies between spectra (Fig. 3 (b)) were minimal, suggesting a negligible impact of temperature on the properties of Au NPs. Thus, conducting Au NPs synthesis at room temperature is both efficient and advantageous in terms of energy and process simplicity. Henceforth, when referencing sample Au NPs, it pertains to those synthesized with a 0.008 g/mL peel extract concentration at room temperature.

### 3.2. Transmission electron microscopy analysis

TEM analysis was utilized to determine the particle size and morphology of all synthesized Au NPs, as illustrated in Fig. 4 along with the corresponding particle size distribution. Fig. 4 (a) to (d) depict the influence of peel extract concentration on Au NPs properties. An increase in concentration from 0.002 g/mL to 0.008 g/mL resulted in the average particle size rising from 12.55 nm to 24.95 nm. This trend aligns with the UV-Visible spectrum, where a red-shift of the maximum absorbance was observed. Further increases to 0.012 g/mL led to a slight



Fig. 2. Image of (a) Peel extract, (b) gold salt solution, (c) Au NPs and (d) proposed formation mechanism of Au NPs.

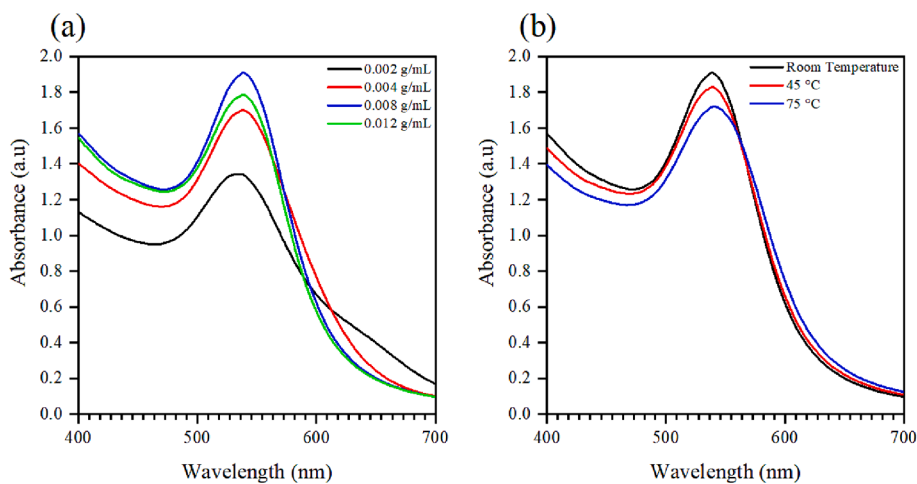


Fig. 3. UV-Visible spectra of Au NPs synthesized with (a) various peel extract concentration and (b) various reaction temperature.

decrease in average particle size to 23.21 nm, possibly due to excess plant extract serving as a capping agent, thereby restraining particle growth. At 0.002 g/mL peel extract concentration, various morphologies such as triangles, spheres, and rods were obtained. However, as the concentration increased, a more consistent spherical shape for the Au NPs was achieved. Adequate plant extract enables the control of Au NPs' crystal growth to attain the desired morphology (Bopape et al., 2022).

Moreover, TEM images (Fig. 4 (c) and (d)) highlight the role of peel extract in capping Au NPs and reducing nanoparticle agglomeration. In summary, the impact of peel extract concentration indicates that a low concentration is sufficient to partially reduce the salt to Au NPs but insufficient to control morphology. The threshold concentration facilitates maximum reduction, ensuring consistency in shape. Beyond this threshold, only minimal reduction in particle size is observed.

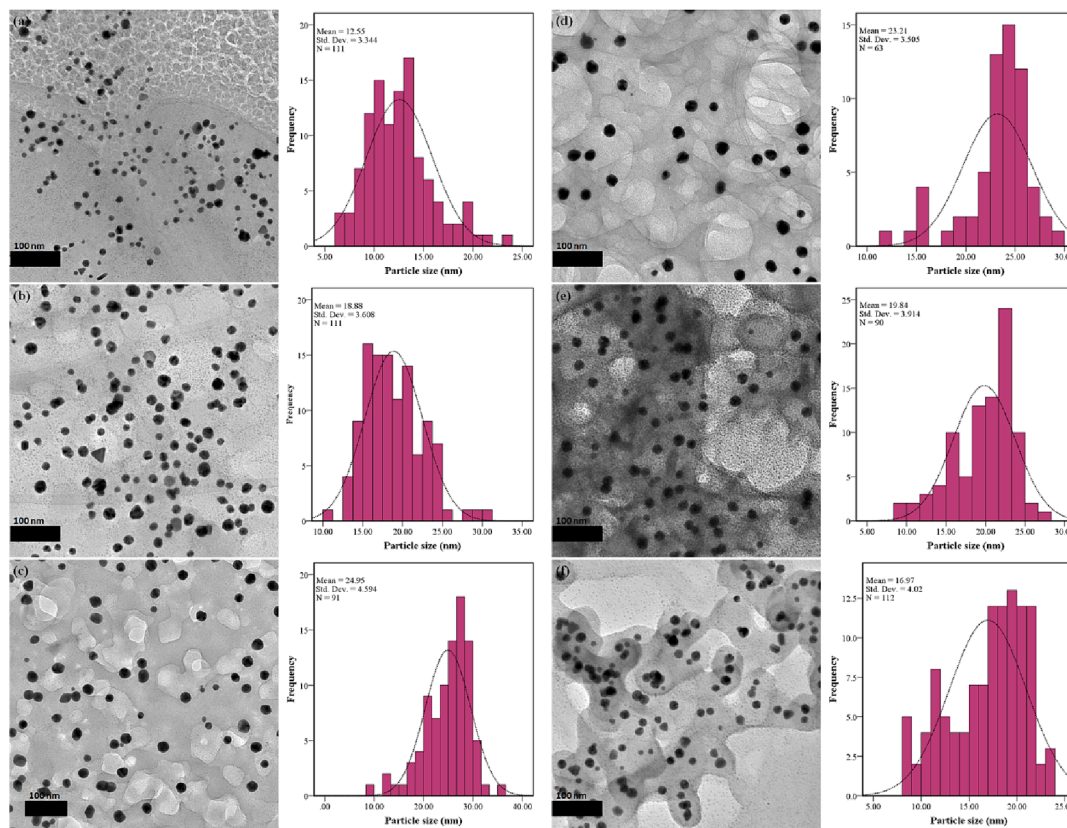


Fig. 4. TEM images of Au NPs synthesized at various conditions. (a) 0.002 g/mL peel extract, (b) 0.004 g/mL peel extract, (c) 0.008 g/mL peel extract, (d) 0.012 g/mL peel extract, (e) 45 °C reaction temperature and (f) 75 °C reaction temperature.

Consequently, a peel extract concentration of 0.008 g/mL emerges as the optimal condition for Au NPs production.

The impact of reaction temperature was investigated, and TEM

images of Au NPs synthesized at 45 °C and 75 °C are depicted in Fig. 4 (e) and (f), respectively. Interestingly, as temperature increased, the average particle size decreased from 19.84 nm to 16.97 nm. This

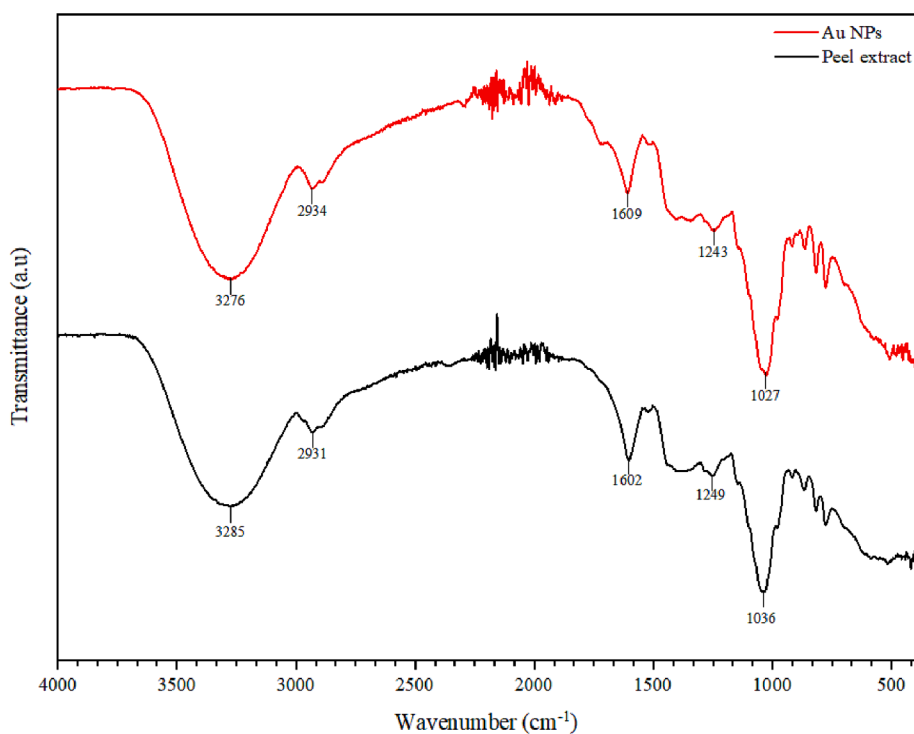


Fig. 5. FTIR spectra of synthesized Au NPs and peel extract.

reduction may be attributed to changes in the behavior of the peel extract. At elevated temperatures, phytochemicals within the extract could undergo reactions enhancing their capping capabilities. The TEM images also indicate complete encapsulation of Au NPs by the plant extract at higher temperatures, unlike at room temperature where encapsulation is less complete. This supports the notion of temperature-induced changes in extract behavior. Additionally, nucleation dominated Au NPs formation at higher temperatures, resulting in smaller particles. While particle shape remained largely unchanged at 45 °C, rod and triangle shapes emerged at 75 °C (Anadozie et al., 2022).

### 3.3. Fourier transform infrared spectroscopy (FTIR) analysis

FTIR analysis was conducted to examine the functional groups involved in facilitating the reduction of gold salt to Au NPs. Fig. 5 displays the spectra of the plant extract and the synthesized Au NPs. In the peel extract, the peak at 3285  $\text{cm}^{-1}$  signifies hydroxyl and amine functional groups. The presence of an amine group is further supported by the peak at 1602  $\text{cm}^{-1}$ , attributed to N-H bend of primary amine (Sivakavinesan et al., 2022). In the region of 1000–1200  $\text{cm}^{-1}$ , the observed bands suggest the existence of carboxylic acids, alcohols and ethers functional groups. These identified functional groups indicate the presence of phenolic and flavonoid phytochemicals in the plant extract (Lim et al., 2015). Analysis of the Au NPs spectrum revealed the presence of all the peaks from the peel extract. However, shifts in the peaks were observed, indicating interactions between the phytochemicals in the peel extract and the synthesized Au NPs, which effectively capped and stabilized the nanoparticles.

### 3.4. X-ray diffraction (XRD) analysis

The crystallinity and purity of the synthesized Au NPs were examined through XRD analysis, as illustrated in Fig. 6, depicting the XRD pattern of both the peel extract and the Au NPs. In the case of the peel extract, a broad peak ranging from 10 to 50° was observed, indicative of its amorphous nature. Notably, a relatively intense peak was noted around 17.91°, possibly attributed to the presence of carbohydrates in

the extract (Ismail et al., 2023). The XRD pattern of Au NPs fits well with the reference pattern, with peaks were observed at 38.30°, 44.43°, 64.82°, 77.91° and 81.84°, corresponding to the planes of (1 1 1), (2 0 0), (2 2 0), (3 1 1) and (2 2 2), respectively (Pechyen et al., 2021). The prominence of the peak at 38.30° suggests its significance as the main orientation of growth (Patil et al., 2023). Furthermore, the Au NPs XRD pattern revealed a broad peak in the range of 2 $\theta$  from 20 to 30°, indicating the presence of peel extract. The observed shifting of peaks suggests an interaction between the Au NPs and the peel extract (Bousalem et al., 2020). The average crystallite size, determined using the Scherrer formula, was found to be 21 nm. These XRD findings closely resemble those reported in previous studies utilizing plant extract in Au NPs synthesis (Al-Radadi, 2022, Shanmugam, 2022, Patil et al., 2023).

### 3.5. Zeta potential analysis

The stability of the synthesized Au NPs was evaluated by determining the zeta potential. To be considered stable, the zeta potential values must either exceed + 30 mV or be lower than -30 mV (Shnoudeh et al., 2019). The zeta potential of the peel extract is -43.42 mV and after the formation of Au NPs using the extract, the zeta potential reduced to -35.74 mV. Despite the reduction, it remains above -30 mV, indicating that the synthesized Au NPs are stable.

### 3.6. Spectral transmittance test results of Au NPs

The utilization of green-synthesized Au NPs as optical filters has received limited research attention to date. This study lays the groundwork for exploring the potential of these plasmonic nanoparticles as optical filters in PVT systems. For silicon and germanium PV cells, an ideal optical filter should transmit wavelengths between 751 to 1126 nm and 1270 to 1906 nm, respectively, with absorption outside these ranges (Hashemian et al., 2022). To assess the potential of green-synthesized Au NPs as optical filters, the transmittance of solutions at various concentrations was recorded, as depicted in Fig. 7 (a), and the average transmittance at specific wavelength ranges was determined, as shown in Fig. 7 (b). Notably, the optical path length was set at 10 mm, with a

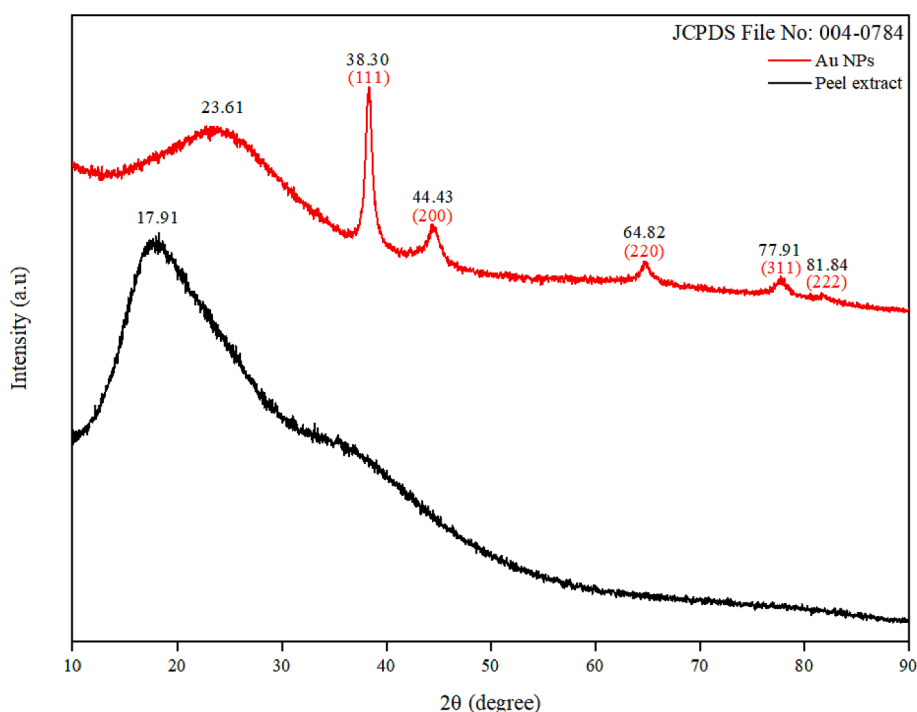
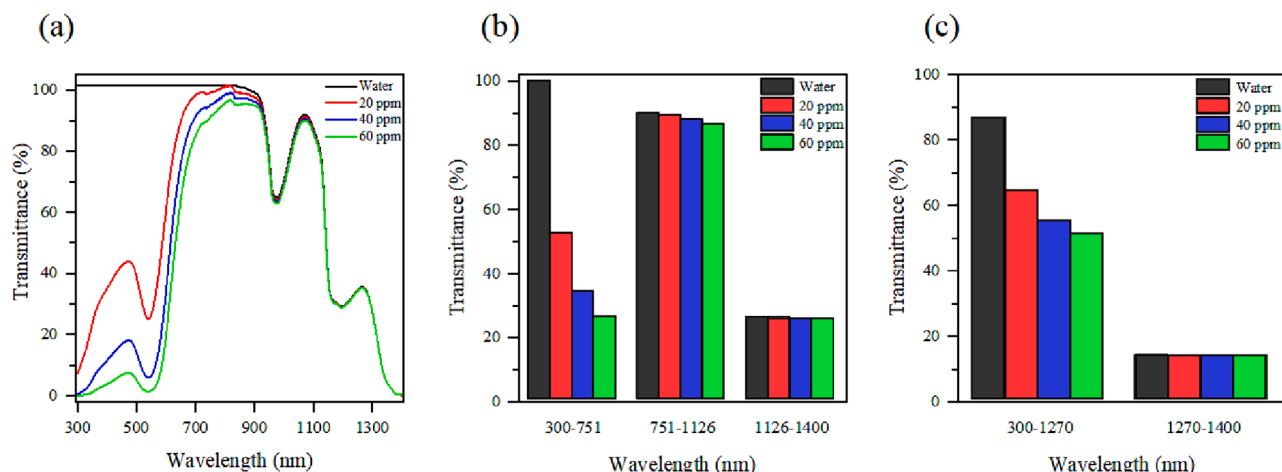


Fig. 6. XRD patterns of Au NPs and peel extract.



**Fig. 7.** (a) Spectral transmittance, (b) average spectral transmittance according to silicon PV cell and (c) average spectral transmittance according to germanium PV cell at different Au NPs concentration.

measurement error of approximately  $\pm 2\%$ . Within the range of 1126–1400 nm, no significant change in transmittance was observed for all samples. However, within the 300–751 nm range, Au NPs solutions exhibited excellent absorption compared to water. Additionally, the absorption band around 300–500 nm was attributed to the plasmonic response of Au NPs (Han et al., 2019). As depicted in Fig. 7 (b), with an increase in Au NPs concentration up to 60 ppm, the average transmittance in the shorter wavelength region reduced to less than 20%, with some absorption occurring in the spectral region of silicon PV cells. However, the transmittance in the desired spectral range (751–1126 nm) remained high, at approximately 87%. These results underscore the promising potential of green-synthesized Au NPs as optical filters for silicon PV cells due to their high transmittance and absorption characteristics. For germanium PV cells, achieving high transmittance within the 1270–1906 nm range is crucial. However, as shown in Fig. 7 (c), transmittance within this range is low, likely due to the properties of the base fluid. Varying the base fluid may improve transmittance and enhance the filtering capability of green-synthesized Au NPs. Between 300 to 1270 nm, transmittance decreases with increasing Au NPs concentration, enabling the absorption and conversion of light energy to thermal energy. Water proves to be a suitable base fluid for silicon PV cells. The potential of synthesized Au NPs for germanium PV cells can be explored by altering the base fluid. It's worth noting that this study assessed filtering capability within the 300–1400 nm range, neglecting higher wavelengths.

### 3.7. Catalytic reduction of rhodamine B

The catalytic activity of the synthesized Au NPs was assessed by reducing rhodamine B dye with  $\text{NaBH}_4$ . Fig. 8 shows the degradation percentage of RhB with and without Au NPs, measured at 554 nm. Within 48 min, Au NPs achieved a maximum degradation of 97%, while without Au NPs, the degradation reached 88% in the same duration. This demonstrates that Au NPs act as catalysts, accelerating the RhB degradation. Calculating pseudo-first order degradation rates revealed a rate of  $0.0795 \text{ min}^{-1}$  with Au NPs and  $0.0445 \text{ min}^{-1}$  without Au NPs. These findings suggest that Au NPs significantly enhanced dye degradation in the presence of  $\text{NaBH}_4$ . Prior research supports these findings (Latha et al., 2018, Sivakavinesan et al., 2022).

## 4. Conclusion

Au NPs were successfully synthesized using *Artocarpus odoratissimus* peel extract as both the reducing and capping agent. The influence of peel extract concentration and reaction temperature on Au NPs

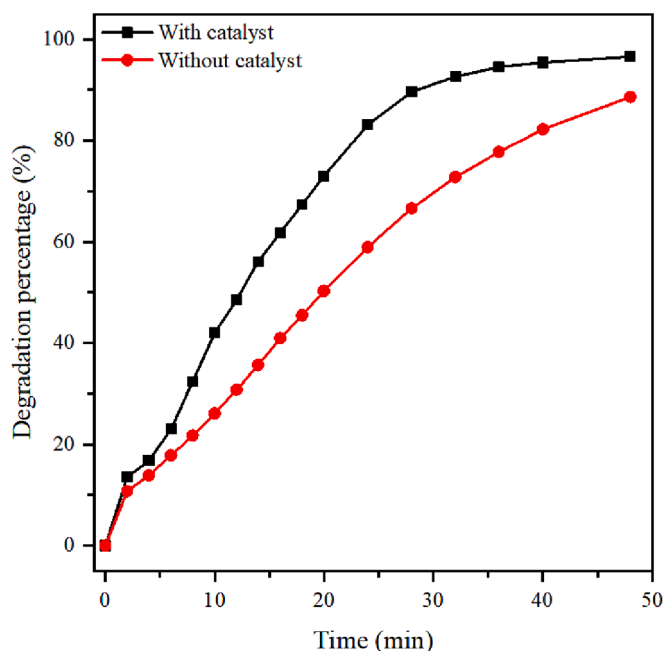


**Fig. 8.** Catalytic degradation percentage of RhB.

properties was investigated through various characterization techniques. Au NPs with the best morphology was obtained within 20 min at room temperature using 0.008 g/mL peel extract concentration, resulting in spherical particles with an average size of 24.95 nm. Optical analysis revealed excellent beam-splitting capabilities for silicon PV cells, with high transmittance within the 751–1126 nm range and significant absorbance at lower wavelengths (300–751 nm). The synthesized Au NPs exhibit potential for use as optical filters for germanium PV cells under different fluid conditions. Additionally, catalytic studies demonstrated the ability of green-synthesized Au NPs to expedite the degradation of RhB dye. This research lays the groundwork for exploring the feasibility of green-synthesized Au NPs in spectral beam-splitting for PVT technology and catalytic degradation applications.

## Funding and acknowledgement

The authors would like to acknowledge the support from the Ministry of Higher Education (MOHE) through the Fundamental Research

Grant Scheme (Ref: FRGS/1/2018/STG07/UTM/02/4 – Fundamental Study into Overcoming the Temperature Paradox in Hybrid Solar Cells), Takasago Research Grant (R.K130000.7343.4B732), Malaysia-Japan International Institute of Technology (MJIT) and Universiti Teknologi Malaysia (UTM) for the funding and opportunity to conduct the research.

### CRedit authorship contribution statement

**Eleen Dayana Mohamed Isa:** Writing – review & editing, Writing – original draft, Visualization, Validation, Methodology, Investigation, Formal analysis, Data curation, Conceptualization. **Siti Rahmah Aid:** Writing – review & editing, Writing – original draft, Supervision, Resources, Project administration, Investigation, Funding acquisition, Formal analysis, Conceptualization. **Roshafima Rasit Ali:** Writing – review & editing, Supervision, Resources, Investigation, Funding acquisition. **Yutaka Asako:** Writing – review & editing, Supervision, Project administration, Methodology, Funding acquisition, Formal analysis, Conceptualization. **Kamyar Shameli:** Writing – review & editing, Supervision, Methodology, Investigation, Formal analysis, Conceptualization. **Nur Farhana Arissa Jonny:** Methodology, Investigation, Formal analysis, Data curation, Conceptualization. **Aina Hiyama Zazuli:** Methodology, Investigation, Formal analysis, Data curation. **Siti Husna Mohd Taib:** Methodology, Investigation, Formal analysis. **Mostafa Yusefi:** Methodology, Investigation.

### Declaration of competing interest

The authors declare that they have no known competing financial interests or personal relationships that could have appeared to influence the work reported in this paper.

### References

- Abid, N., Khan, A.M., Shujait, S., et al., 2022. Synthesis of nanomaterials using various top-down and bottom-up approaches, influencing factors, advantages, and disadvantages: A review. *Adv. Colloid Interface Sci.* 300, 102597 <https://doi.org/10.1016/j.cis.2021.102597>.
- Abu Bakar, F. I. and M. F. Abu Bakar, 2018. *Tarap—Artocarpus odoratissimus*. Exotic Fruits. S. Rodrigues, E. de Oliveira Silva and E. S. de Brito, Academic Press: 413–418.
- Abu Bakar, M.F., Karim, F.A., Perisamy, E., 2015. Comparison of Phytochemicals and Antioxidant Properties of Different Fruit Parts of Selected Artocarpus Species from Sabah. *Malaysia. Sains Malaysiana.* 44 (3), 355–363. <https://doi.org/10.17576/jsm-2015-4403-06>.
- Al-Radadi, N.S., 2022. Single-step green synthesis of gold conjugated polyphenol nanoparticle using extracts of Saudi's myrrh: Their characterization, molecular docking and essential biological applications. *Saudi Pharm. J.* 30 (9), 1215–1242. <https://doi.org/10.1016/j.jsps.2022.06.028>.
- Alvarado, M.C., 2023. Marang fruit (*Artocarpus Odoratissimus*) waste: A promising resource for food and diverse applications: A review of its current status, research opportunities, and future prospects. *Food Bioeng.* 2 (4), 350–359. <https://doi.org/10.1002/fbe.2.12065>.
- Anadozie, S.O., Adewale, O.B., Fadaka, A.O., et al., 2022. Synthesis of gold nanoparticles using extract of *Carica papaya* fruit: Evaluation of its antioxidant properties and effect on colorectal and breast cancer cells. *Biocatal. Agric. Biotechnol.* 42, 102348 <https://doi.org/10.1016/j.bcab.2022.102348>.
- Fadzelly Abu Bakar, M., M. Mohamed, A. Rahmat, et al., 2010. Cytotoxicity and polyphenol diversity in selected parts of and fruits. *Nutr. Food Sci.* 40 (1) 29–38. DOI: 10.1108/00346651011015890.
- Bopape, D.A., Motaung, D.E., Hintsho-Mbita, N.C., 2022. Green synthesis of ZnO: Effect of plant concentration on the morphology, optical properties and photodegradation of dyes and antibiotics in wastewater. *Optik.* 251, 168459 <https://doi.org/10.1016/j.jijleo.2021.168459>.
- Bousalem, S., Zeggai, F.Z., Baltach, H., et al., 2020. Physical and electrochemical investigations on hybrid materials synthesized by polyaniline with various amounts of ZnO nanoparticle. *Chem. Phys. Lett.* 741 <https://doi.org/10.1016/j.cplett.2020.137095>.
- Cortez-Valadez, M., Ramirez-Rodriguez, L.P., Martinez-Suarez, F., et al., 2021. Green Synthesis up to Geometric Gold Microparticles. *J. Inorg. Organomet. Polym. Mater.* 31 (3), 1079–1085. <https://doi.org/10.1007/s10904-020-01721-4>.
- Das, U., Biswas, R., 2023. Unravelling optical properties and morphology of plasmonic gold nanoparticles synthesized via a novel green route. *Chem. Pap.* 77 (6), 3485–3493. <https://doi.org/10.1007/s11696-023-02716-4>.
- Duan, H., Zheng, Y., Xu, C., et al., 2019. Experimental investigation on the plasmonic blended nanofluid for efficient solar absorption. *Appl. Therm. Eng.* 161, 114192 <https://doi.org/10.1016/j.applthermaleng.2019.114192>.
- Han, X., Chen, X., Wang, Q., et al., 2019. Investigation of CoSO<sub>4</sub>-based Ag nanofluids as spectral beam splitters for hybrid PV/T applications. *SoEn.* 177, 387–394. <https://doi.org/10.1016/j.solener.2018.11.037>.
- Han, X., Zhao, X., Huang, J., et al., 2022. Optical properties optimization of plasmonic nanofluid to enhance the performance of spectral splitting photovoltaic/thermal systems. *Renew. Energy* 188, 573–587. <https://doi.org/10.1016/j.renene.2022.02.046>.
- Hashemian, M., Jafarmadar, S., Khalilarya, S., et al., 2022. Energy harvesting feasibility from photovoltaic/thermal (PV/T) hybrid system with Ag/Cr<sub>2</sub>O<sub>3</sub>-glycerol nanofluid optical filter. *Renew. Energy* 198, 426–439. <https://doi.org/10.1016/j.renene.2022.07.153>.
- Ismail, H.A., Ramaiya, S.D., Zakaria, M.H., 2023. Compositional Characteristics and Nutritional Quality of Indigenous Fruit of *Artocarpus odoratissimus* Blanco. *Malays. Appl. Biol.* 52 (5), 187–203. <https://doi.org/10.55230/mabjournal.v52i5.icf1c15>.
- Kamyar, S., Siti Rahmah, A., Nur Farhana Arissa, J., et al., 2021. Green Synthesis of Gold Nanoparticles Based on Plant Extract for Nanofluid-based Hybrid Photovoltaic System Application. *J. Res. Nanosci. Nanotechnol.* 4 (1), 19–34. <https://doi.org/10.37934/jrn.4.1.1934>.
- Kumar, S., Chander, N., Gupta, V.K., et al., 2021. Progress, challenges and future prospects of plasmonic nanofluid based direct absorption solar collectors – A state-of-the-art review. *SoEn.* 227, 365–425. <https://doi.org/10.1016/j.solener.2021.09.008>.
- Latha, D., Prabu, P., Gnanamoorthy, G., et al., 2018. Size-dependent catalytic property of gold nanoparticle mediated by *Justicia adhatoda* leaf extract. *SN Appl. Sci.* 1 (1), 134. <https://doi.org/10.1007/s42452-018-0148-y>.
- Lee, K.X., Shameli, K., Miyake, M., et al., 2017. Gold Nanoparticles Biosynthesis: A Simple Route for Control Size Using Waste Peel Extract. *IEEE Trans. Nanotechnol.* 16 (6), 954–957. <https://doi.org/10.1109/tmano.2017.2728600>.
- Lee, K.X., Shameli, K., Mohamad, S.E., et al., 2019. Bio-Mediated Synthesis and Characterisation of Silver Nanocarrier, and Its Potent Anticancer Action. *Nanomaterials* 9 (10). <https://doi.org/10.3390/nano9101423>.
- Lim, L.B.L., Priyantha, N., Zehra, T., et al., 2015. Adsorption of crystal violet dye from aqueous solution onto chemically treated *Artocarpus odoratissimus* skin: equilibrium, thermodynamics, and kinetics studies. *Desalin. Water Treat.* 57 (22), 10246–10260. <https://doi.org/10.1080/19443994.2015.1033474>.
- Nayak, S., Goveas, L.C., Selvaraj, R., et al., 2022. Use of *Cyclea peltata* mediated gold nanospheres for adsorptive degradation of methyl green dye. *Biore. Technol. Rep.* 20, 101261 <https://doi.org/10.1016/j.biteb.2022.101261>.
- Patil, T.P., Vibhute, A.A., Patil, S.L., et al., 2023. Green synthesis of gold nanoparticles via *Capsicum annum* fruit extract: Characterization, antiangiogenic, antioxidant and anti-inflammatory activities. *Appl. Surf. Sci. Adv.* 13, 100372 <https://doi.org/10.1016/j.apsadv.2023.100372>.
- Pechyen, C., Ponsanti, K., Tangnorawich, B., et al., 2021. Waste fruit peel – Mediated green synthesis of biocompatible gold nanoparticles. *J. Mater. Res. Technol.* 14, 2982–2991. <https://doi.org/10.1016/j.jmrt.2021.08.111>.
- Punnoose, M.S., Joseph, S., John, B.K., et al., 2022. Antibacterial, Cytotoxic, and Catalytic Potential of Aqueous *Amaranthus tricolor*-Mediated Green Gold Nanoparticles. *Plasmonics.* 17 (4), 1387–1402. <https://doi.org/10.1007/s11468-022-01622-x>.
- Punnoose, M.S., Mathew, B., 2022. Microwave-assisted green synthesis of *Cyanthillium cinereum* mediated gold nanoparticles: Evaluation of its antibacterial, anticancer and catalytic degradation efficacy. *Res. Chem. Intermed.* 48 (3), 1025–1044. <https://doi.org/10.1007/s11164-021-04641-1>.
- Rokkarukala, S., Cherian, T., Ragavendran, C., et al., 2023. One-pot green synthesis of gold nanoparticles using *Sarcophyton crassocaule*, a marine soft coral: Assessing biological potentialities of antibacterial, antioxidant, anti-diabetic and catalytic degradation of toxic organic pollutants. *Heliyon.* 9 (3), e14668.
- Shanmugam, P., 2022. Green route synthesis of *alpinia calcarata* functionalized gold nanoparticles for nonlinear optical applications. *Heliyon.* 8 (8), e10409.
- Shnoudeh, A.J., Hamad, I., Abdo, R.W., et al., 2019. Chapter 15 - Synthesis, Characterization, and Applications of Metal Nanoparticles. In: Tekade, R.K. (Ed.), *Biomaterials and Bionanotechnology*. Academic Press, pp. 527–612.
- Sivakavinesan, M., Vanaja, M., Lateef, R., et al., 2022. Citrus *limetta* Risso peel mediated green synthesis of gold nanoparticles and its antioxidant and catalytic activity. *J. King Saud Univ. Sci.* 34 (7), 102235 <https://doi.org/10.1016/j.jksus.2022.102235>.
- Taylor, R.A., Otanicar, T., Rosengarten, G., 2012. Nanofluid-based optical filter optimization for PV/T systems. *Light Sci. Appl.* 1 (10), e34–e. <https://doi.org/10.1038/lsa.2012.34>.
- Wu, X., Chen, G.Y., Owens, G., et al., 2019. Photothermal materials: A key platform enabling highly efficient water evaporation driven by solar energy. *Mater. Today Energy* 12, 277–296. <https://doi.org/10.1016/j.mtener.2019.02.001>.
- Xia, X., Cao, X., Li, N., et al., 2023. Study on a spectral splitting photovoltaic/thermal system based on CNT/Ag mixed nanofluids. *Energy* 271, 127093. <https://doi.org/10.1016/j.energy.2023.127093>.
- Yulianti, I., Padlilah, R., Ariyanti, R., et al., 2022. Mapping review of the potential of Tarap Plants (*Artocarpus odoratissimus*) for health. *Int. J. Health Sci.* 2351–2357 <https://doi.org/10.53730/ijhs.v6nS4.7062>.